Available online at www.sciencedirect.com
ScienceDirect
Minerals Engineering 21 (2008) 83–92
MINERALS ENGINEERING
This article is also available online at: www.elsevier.com/locate/mineng

Surface chemistry fundamentals of biosorption of *Rhodococcus opacus* and its effect in calcite and magnesite flotation

Ana Elisa C. Botero [a,*], Maurício Leonardo Torem [b], Luciana Maria S. de Mesquita [c]

[a] *Pontifical Catholic Bolivarian University, Chemical Engineering, Circular 1 No. 70-01 Laureles Medellin, Antioquia, Colombia*
[b] *Department of Materials Science, Metallurgycatholic University, Rio de Janeiro, Brazil*
[c] *Brazilian Petroleum Agency, Rio de Janeiro, Brazil*

Received 22 May 2007; accepted 29 August 2007
Available online 1 November 2007

Abstract

The affinity of *Rhodococcus opacus* cells for calcite and magnesite surfaces has been studied in order to evaluate its application as a flotation collector. The surface properties of minerals and *R. opacus* were characterized using infrared techniques. The mineral spectrums, before and after the bacterial interaction, indicated a mineral surface interaction with the *R. opacus* cell wall. The results were compared with the zeta potential curves as a function of the pH. The cell wall composition of *R. opacus* was characterized and the *R. opacus* hydrophobicity was either evaluated with contact angle measurements. The interfacial tension components were calculated based on the van Oss and Fowkes equations. The obtained results were supported by DLVO and X-DLVO theories for selected pH values. The results show the paramount innovation that *R. opacus* presents as a biocollector and its possible application in the mineral flotation industry.
© 2007 Elsevier Ltd. All rights reserved.

Keywords: Bioflotation; Adsorption; *Rhodococcus opacus*; Industrial minerals; DLVO and X-DLVO theory

1. Introduction

Bioflotation uses micro-organisms as friendly modifiers, collectors and depressants. These micro-organisms may act as bioreagents and induce hydrophobic properties once they can adhere selectively onto the mineral surface (Sharma and Hunumantha Rao, 2002). In recent years, the bacterial affinity for the mineral surface has been studied and several works have been carried out in order to evaluate the micro-organisms behavior and their interaction with mineral surfaces (Sharma, 2001).

The micro-organism cell surface is conformed by functional groups like polymers, peptides, proteins and micolic acids (Van der Wal et al., 1997). These groups must adhere to the mineral surface directly and utilize cell surface associated or extracellular biopolymers to catalyze chemical reactions on the mineral surface (Chandaphara et al., 2006). Like traditional reagents, a micro-organism interacts with the mineral surface and gives amphoteric characteristics to it (Mesquita et al., 2003). Some micro-organisms like *Bacillus polymyxa*, *Mycobacterium phei*, *Rhodococcus opacus*, *B. subtillis*, *Thiobacillus ferroxidans* and *Aspergillus niger* have been used as bioreagents for the separation of different mineral systems (Deo and Natarajan, 1999; Misra et al., 1996; Dubel et al., 1992; Mesquita, 2000; Zheng et al., 2001; Hosseini et al., 2005; Gawel et al., 1997).

Application of bioreagents as collectors invokes several fundamental aspects: surface charge, presence of specific hydrophobic groups and polymers compounds which deeply affect their adhesion to the mineral (Pearse, 2005; Smith and Miettinem, 2006). Therefore, for mineral bioflotation, it is very important to understand the microbial surface characteristics and its behavior onto the mineral surface (Poortiga et al., 2002; Van der Mei et al., 1998).

* Corresponding author. Tel.: +55 21 35271723.
E-mail addresses: ana.casas@upb.edu.co (A.E.C. Botero), torem@dcmm.puc-rio.br (M.L. Torem), lmesquita@anp.gov.br (L.M.S. de Mesquita).

0892-6875/$ - see front matter © 2007 Elsevier Ltd. All rights reserved.
doi:10.1016/j.mineng.2007.08.019

The hydrophobic behavior is associated with the bacterial species and may change depending on the functional groups, specially the presence of lipidic and proteic groups associated with the cell wall (Sharma, 2001; Van Oss, 1995). Several methods have been used for establishing the hydrophobic character in the bacterial cell wall. The hydrophobicity can be established by bacterial affinity for polar solvents, by thin chromatography or by contact angle measurements (Fröberg et al., 1999; Van Oss, 1994). Van der Mei et al. (1998) measured the contact angle for 142 microbial species (bacteria, yeast and actinomycetes). Furthermore, they found that the contact angle values have correlation with the hydrophobicity extent and varies between 15° and 110°. Sharma and Hunumantha Rao (2002) evaluated the surface energy of microbial cells using the contact angle values and different thermodynamics approaches.

The bacterial adhesion onto the mineral surface can be sustained using the DLVO and the X-DLVO theories as a function of the distance and the thermodynamic approach (Hermansson, 1999). The theories may predict how the total interaction energy between the cell wall and the mineral surface is established (Van Oss, 1994; Israelachvili, 1995).

The DLVO theory may consider the interaction between cells and mineral particles as the balance of van der Waals attractive forces and repulsive forces by electronic clouds as a function of the distance in between the particles (Israelachvili, 1995; Laskowski and Ralston, 1992). The electrostatic interactions are due to the charge of two particles, when immersed in a polar liquid such as water (Van Oss, 1994). The van der Waals interactions between surfaces depend on the Hamaker constant of the particle–particle system and can be estimated with the Fowkes approximation and the Lifshitz–van der Waals surface tension components (Van Oss, 1994; Kwok and Neumann, 1999).

The extended DLVO theory considers that the total forces can be affected by specific characteristics such as roughness, pilis, steric effects, acid–base interaction and hydrophobic and hydrophilic effects. These characteristics can affect the total interaction energy between cells and particles. The acid–base (AB) interactions are based on electron-donating and electron-accepting interactions and can be evaluated using the LW–AB approach and the AB surface tension components (Hermansson, 1999).

The thermodynamic approach compares the interfacial free energy on the interacting forces before and after adhesion (Sharma, 2001).

The *R. opacus* is a unicellular gram positive bacteria with different types of compounds on their surface. This micro-organism has polysaccharides, carboxylic acids, lipid groups and micolic acids in the cell wall that gives an amphoteric behavior on the cell surface (Mesquita, 2000; Stratton et al., 2002). Considering the literature about the interaction of micro-organisms with the mineral surfaces (Sharma, 2001; Smith and Miettinem, 2006; Chandaphara et al., 2006; Natarajan, 2006; Vijayalaskhmi and Raichur, 2003), one can realize that there are few studies on the use of *R. opacus* as a biocollector in the mineral processing research. The total interaction forces of *R. opacus* – hematite and *R. opacus* – quartz system using the DLVO classic theory was previously studied by Mesquita et al. (2003). The results obtained showing a strong interaction between cells and minerals particles, mainly for hematite.

The aim of this paper is to contribute for a better understanding on the fundamentals of bioflotation using a hydrophobic bacteria applied to two relevant industrial Brazilian minerals as magnesite and calcite. The DLVO and X-DLVO theories and the thermodynamic approach were used as an innovator tool to evaluate the interaction between *R. opacus* cells and the calcite and magnesite particles and substantiate the experimental results.

2. Materials and methods

2.1. Minerals preparation

Pure calcite and magnesite mineral samples were provided by the Centre for Mineral Technology (CETEM) and Magnesite S.A., respectively. The samples were properly ground and sieved for the experimental procedures as shown in Table 1. The detailed experimental procedure is described elsewhere (Mesquita, 2000).

2.2. Micro-organisms, media and growth

R. opacus strain was obtained from Fundação André Tossello Institute (São Paulo, Brazil). It was sub-cultured in the laboratory using a *Streptomyces* liquid medium (SM) with 10.0 g dm^{-3} glucose, 5.0 g dm^{-3} peptone, 5.0 g dm^{-3} malt extract, 2.5 g dm^{-3} yeast extract and 1.0 g dm^{-3} $CaCO_3$. After 48 h of incubation on a rotary shaker at 28 °C, the culture was centrifuged and washed with deionized water. The cells were suspended in a 0.01 M NaCl solution. Concentration of the cellular suspension was quantified by dry weight curve.

2.3. Determination of cell wall associated polysaccharides, lipids and proteins

The *R. opacus* cells were washed and the cell wall associated material was extracted with 0.01 M phosphate buffer solution at pH 7.30 dm^{-3} of this cell suspension and 30 dm^{-3} of EDTA 2% were mixed and after 2 h at 4 °C, the solution was centrifuged and the supernatant was collected. The method of cell wall associated components extraction was described by Cammarota (1998).

Table 1
Mean size particle (d_{80}) for the experimental work

Experimental work	Mean size particle
Zeta potential evaluation	37.0 (μm)
Adhesion tests	74.0 (μm)
Microflotation experiments	106.0 (μm)
Contact angle measurements samples	1.0 × 1.0 × 2.0 (cm)

The cell wall associated lipids were extracted with methanol and hexane, the organic phase was weighed. The cell wall associated polysaccharides were measured using the phenol–sulfuric acid method (Dubois et al., 1956) and the cell wall associated protein with the Lowry method (Lowry et al., 1951). The polysaccharides, lipids, and proteins were reported as a percentage of the weighed total *R. opacus* cells.

2.4. Zeta potential evaluation

Zeta potential measurements for *R. opacus* cells, calcite and magnesite were carried out on a micro-electrophoresis apparatus zeta meter system 3.0+. The concentration of the mineral and biomass suspension were both of 100 mg dm^{-3}. The cells concentration was selected based on previous studies (Botero et al., 2006, 2007); NaCl 0.01 M was used as an indifferent electrolyte. The isoelectric point (IEP) of pure calcite and magnesite minerals and *R. opacus* suspension were evaluated. The evaluation of zeta potential profiles for calcite and magnesite were also carried out in the absence and presence of *R. opacus*.

2.5. Fourier transformed infrared spectroscopy (FTIR)

Infrared absorption spectra were recorded on a Nicolet FTIR 2000 spectrophotometer; a KBr matrix was used as reference and a deuterated triglycine sulphate (DTGS) as detector. The data acquisition was carried out through the transmission mode. The spectra of calcite and magnesite, before and after the *R. opacus* interaction, were evaluated.

The *R. opacus* cell suspension and the minerals samples were filtered and dried at 75 °C. The dried powder was properly mixed in a KBr matrix. The spectra were collected after 120 scans at 4 cm^{-1}.

2.6. Microflotation experiments

The microflotation assays were carried out in a modified Hallimond tube. An amount of 0.8 g of mineral was added to 0.17 dm^{-3} total volume suspension; the pH was adjusted with 0.1 M of HCl or NaOH solution. A variable concentration of *R. opacus* solution was added. The bioreagent was conditioned onto the suspension for 10 min. Ten minutes was the flotation time adopted and the air flow 50×10^{-3} dm^{-3} min^{-1}.

The floated and unfloated minerals were thoroughly washed, filtered and weighed. The floatability was then calculated as the ratio of floated and unfloated minerals and the total weighed mineral (floated and unfloated).

2.7. Contact angles measurements

The acquisition of static contact angles values were carried out with a Goniometer model 100-00-115 Ramé–Hart. The surface of each mineral sample was carefully polished. The *R. opacus* cells suspension was filtered through a 0.45 μm cellulose triacetate filter paper to obtain the homogeneous bacterial lawn. The detailed experimental procedure is described elsewhere (Van Oss, 1994).

According with the method described by Kwok and Neumann (1999) and Médout-Marère et al. (1998), the different values of contact angles for *R. opacus*, calcite and magnesite were obtained with two polar liquids (water and formamide) and one apolar liquid (α-bromonaftalene). The droop size used was 2×10^{-6} dm^{-3}. The contact angle measurements and the van Oss equation were used to estimate the surface tension components. The Mathcad 13 software was used to solve the equation systems.

2.8. Estimation of interaction energies

The classical DLVO theory considers the total interactions as the summation of electrostatic repulsive forces and London van der Waals attractive forces (Hermansson, 1999).

Considering the *R. opacus* shape as a sphere and the minerals surface as a flat plane, the contribution of electrostatic interaction between them is given by

$$\Delta G_{\mathrm{elt}} = \pi\varepsilon_0\varepsilon a\left\{2\zeta_1\zeta_2 \ln\frac{(1+\mathrm{e}^{(-kH)})}{(1-\mathrm{e}^{(-kH)})} + (\zeta_1^2+\zeta_2^2)\ln(1-\mathrm{e}^{(-2kH)})\right\}, \quad (1)$$

where ε_0 is the permissivity under vacuum 8.85×10^{-12} (C^2 J^{-1} m^{-1}), ε is the dielectric constant of the medium 79; a is the equivalent radius of the *R. opacus* cell 1.24×10^{-6} (m); ξ_1 and ξ_2 are the values of the zeta potential for microbial cell and mineral particle, respectively, (V); $1/k$ is the Debye–Hückel length (nm); H is the distance between the particle and microbial cell surface (nm).

van der Waals attractive forces are given by

$$\Delta G_{\mathrm{ATR}} = -\frac{A_{\mathrm{bwm}}}{6}\left[\frac{a}{H}+\frac{a}{H+2a}+\ln\left(\frac{H}{H+2a}\right)\right], \quad (2)$$

where A_{bwm} is the Hamaker constant for the system bacteria–water–mineral, which in turn is given by

$$A_{\mathrm{bwm}} = [(A_{\mathrm{m}})^{0.5} - (A_{\mathrm{w}})^{0.5}][(A_{\mathrm{b}})^{0.5} - (A_{\mathrm{w}})^{0.5}]. \quad (3)$$

The Hamaker constant for the *R. opacus* and the mineral particles were obtained by contact angle measurements and the following equation:

$$A_{11} = 6\pi r^2 \gamma_{\mathrm{s}}^{\mathrm{d}}, \quad (4)$$

where r represents intermolecular distance and $\gamma_{\mathrm{s}}^{\mathrm{d}}$ is the dispersion component of the surface free energy of the solid. In water and systems with elements such as metal atoms, CH_2 and CH groups, which have nearly the same size, the valor of $6\pi r^2$ can be taken as 1.44×10^{-18} m^2 (Van Oss, 1994).

The γ_s^d can be obtained from the contact angles values for *R. opacus*, magnesite and calcite surfaces using one apolar liquid (α-bromonapthalene) and the Fowkes equation

$$\cos\Theta = -1 + 2\sqrt{\gamma_s^d}\frac{\sqrt{\gamma_l^d}}{\gamma_l}, \quad (5)$$

where Θ represents the contact angle values of the solid surfaces and γ_l, γ_l^d are the liquid surface energy values.

According with Fowkes approach, the surface energies γ_l^d and γ_l for apolar liquid are equals. For α-bromonapthalene the γ_l^d and the γ_l surface energy values are 44.4 (mJ m^{-2}).

After evaluating the individual Hamaker constant for *R. opacus*, calcite and magnesite, the effective Hamaker constant were calculated using Eqs. (3)–(5).

The thermodynamic approach considers the total energy ΔG_{adh} is due by

$$\Delta G_{adh} = \Delta G_{adh}^{LW} + \Delta G_{adh}^{AB}. \quad (6)$$

According with the LW–AB approach the Lifshitz–van der Waals component is given by

$$\Delta G_{adh}^{LW} = -2\left(\sqrt{\gamma_{bv}^{LW}} - \sqrt{\gamma_{wv}^{LW}}\right)\left(\sqrt{\gamma_{mv}^{LW}} - \sqrt{\gamma_{wv}^{LW}}\right), \quad (7)$$

where γ_{bv}^{LW}, γ_{mv}^{LW}, γ_{wv}^{LW} are the Lifshitz–van der Waals interfacial free energy for *R. opacus*, minerals and water, respectively. The interfacial component can be calculated using the contact angle values with an apolar solvent (α-bromonapthalene) and the van Oss equation

$$(1+\cos\Theta)\gamma_l = 2\left(\sqrt{\gamma_s^{LW}\gamma_l^{LW}}\right). \quad (8)$$

The acid base component is calculated by the following expression:

$$\Delta G_{adh}^{AB} = 2\left(\sqrt{\gamma_{bv}^{+}} - \sqrt{\gamma_{mv}^{+}}\right)\left(\sqrt{\gamma_{bv}^{-}} - \sqrt{\gamma_{mv}^{-}}\right) - 2\left(\sqrt{\gamma_{bv}^{+}} - \sqrt{\gamma_{wv}^{+}}\right)\left(\sqrt{\gamma_{bv}^{-}} - \sqrt{\gamma_{wv}^{-}}\right), \quad (9)$$

where γ_{bv}^{+}, γ_{bv}^{-}, γ_{mv}^{+}, γ_{mv}^{-}, γ_{wv}^{+} and γ_{wv}^{-} are acid–base interfacial free energy for *R. opacus* (b), minerals (m) and water (w), respectively. The interfacial components can be calculated using the contact angle values with two polar solvent (water and formamide), the Lifshitz–van der Waals components and the van Oss equation

$$(1+\cos\Theta)\gamma_l = 2\left(\sqrt{\gamma_s^{LW}\gamma_l^{LW}}\right) + 2\left(\sqrt{\gamma_s^{+}\gamma_l^{-}} + \sqrt{\gamma_s^{-}\gamma_l^{+}}\right). \quad (10)$$

The X-DLVO considers the acid–base interaction energy and it is represented by

$$\Delta G^{AB} = \pi a\lambda\Delta G_{adh}^{AB} e^{\frac{(d_0-H)}{\lambda}}, \quad (11)$$

where d_0 is the minimum separation distance between two surfaces (1.57 Å), λ is the correlation length of molecules in liquid (≅6 Å) and ΔG_{adh}^{AB} is calculated with the expression (9).

3. Results and discussion

3.1. Zeta potential evaluation

Fig. 1 shows the zeta potential curves of *R. opacus*, calcite and magnesite as pH function before and after of the interaction with the *R. opacus*.

The IEP value of *R. opacus* was around 3.2, the result was in good accordance with Mesquita et al. (2003). The acidic IEP value of *R. opacus* could be due to the presence of anionic groups on the wall that dominate over the cationic groups. The presence of polysaccharides, phosphates and amino groups on the cell wall give a net charge on the surface that depending on the pH (Poortiga et al., 2002). The charge in the bacterial wall is determined by the dissociation or protonation of these acidic and basic groups. This seems to be a general phenomenon and it is in agreement with the observation depicting that most bacterial cells have isoelectric points below pH 4 (Van der Wal et al., 1997). The zeta potential values were more negative for the pH range above the IEP.

According to Rijnaarts et al. (1995), an IEP pH 2.0 and 2.8 results from a cell surface predominated by glucorinic acids or other polysaccharide associated carboxyl groups. An IEP rather than or equal to pH 3.0 are difficult to interpret, they may reflect mixed contributions of protein or peptidoglican associated $COOH^-$ or NH_3^+ and may results from a combination of NH_3^+ contain polymers and low pK_a anionic polysaccharides contain phosphate and or carboxyl groups.

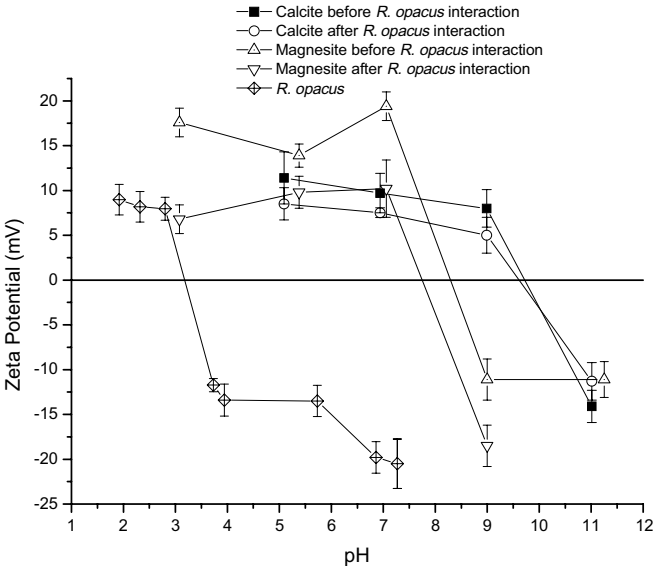

Fig. 1. Zeta potential curves of *R. opacus*, calcite and magnesite as pH function before and after *R. opacus* interaction – NaCl 0.01 M as background electrolyte.

The obtained zeta potential curves for calcite and magnesite as a function of pH are in accordance with equivalent studies by Pokrovsky et al. (1999) and Vdovic and Bigdan (1998) where the IEP values were around 8.2 and 10.0 for magnesite and calcite, respectively.

Observing Fig. 1, it is interesting to become aware of the zeta potential alteration profiles after the bacterial contact with both minerals surfaces. The change could be due to secretion of proteic bacterial compounds that interact with the minerals surfaces. The results are in agreement with those obtained by Deo and Natarajan that found changes on the charges values of the calcite using the *B. polymyxa* as bioreagent (Deo and Natarajan, 1997).

The IEP displacement for magnesite was more significant than for calcite after the *R. opacus* interaction. This behavior would suggest a stronger affinity of *R. opacus* cell for magnesite surface. A similar observation was made by Patra and Natarajan (2003) for a pyrite/mineral gangue system using *B. polymyxa* cells as a bioreagent.

3.2. FTIR and cell wall analysis and determination of cell wall associated polysaccharides, lipids and proteins

The micro-organism cell surface is conformed by functional groups like polymers, peptides, proteins and micolic acids (Van der Wal et al., 1997). Several methods may be used to determinate these groups associated with the bacterial cell wall. Table 2 shows the results of cell wall associated composition according to the Cammarota method, 1998.

The *R. opacus* cell is a gram positive bacteria and the cell wall is composed principally by proteins, enzymes, peptidoglycan and micolic acids (Stratton et al., 2002). The results of cell wall composition show the high proportion of lipids and carbohydrates associated to the *R. opacus*. These compounds may integrate the functional groups presents on the cell wall. The results were compared with the *R. opacus* cell FTIR analysis.

According to the literature (Sharma, 2001; Parker, 1971), the bands, obtained in the FTIR spectra of bacterial cells correspond to characteristic functional groups of the cell wall. Table 3 presents the absorbance bands and the assigned functional groups.

Fig. 2 shows the FTIR spectra of *R. opacus* cell and the absorbance bands obtained. The FTIR spectra obtained showed the presence of CH, CH_2, CH_3, NH, NH_2, NH_3 COOH and CONH groups on the surface of the *R. opacus* cells. The groups obtained are presented in any proteic molecule (Parker, 1971; Deo et al., 2001).

Table 2
Rhodococcus opacus cell wall composition

Cell wall material	Concentration (g dm^{-3})	Composition (%)
Proteins	0.16	2.85
Carbohydrates	0.61	10.54
Lipids	1.92	33.33
Cell suspension	11.52	

Table 3
Absorbance bands and the characteristic functional groups (Sharma, 2001)

Wave number (cm^{-1})	Assigned functional group
3020–2800	Alkyl hydrocarbon
2959, 2934 and 2875	Asymmetric CH_3 stretching, asymmetric CH_2 and symmetric CH_2 stretching
Strong band near 3298 and weaker band at 3072	Asymmetric and symmetric stretching of NH_2
Very intense bands between 1750 and 1620	C=O
Intense sharp band at 1655	Amide group (amide I band)
The band near 1700	–C=O group
1682	NH_2 bending of the primary amide groups or $–NH_3$ of the amine acids
The bands at 1452 and 1390	CH_3 and CH_2
1236	CH_3 wagging modes
1080	$–CH_3$ rocking and CH_2 wagging modes

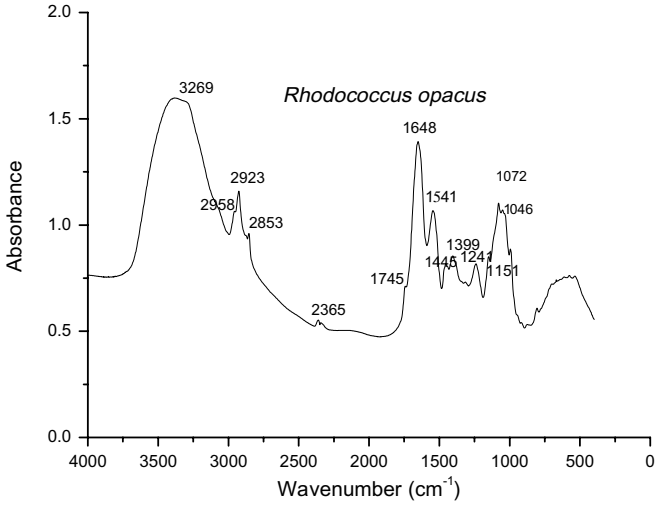

Fig. 2. FTIR spectra of *R. opacus* cells and the principal bands obtained.

The *R. opacus* FTIR spectra are in agreement with the zeta potential and the cell wall composition results. The IEP of *R. opacus* reflects a combination of with NH_3^+ polymers and low pK_a anionic polysaccharides with phosphate and carboxyl groups, which are associated with proteins, lipids and carbohydrates of the cell wall.

Figs. 3 and 4 show the FTIR spectra of magnesite and calcite, respectively, and the principal bands obtained before and after of *R. opacus* interaction.

The FTIR spectra for magnesite and calcite, obtained before the *R. opacus* interaction, show the characteristics bands for carbonates. Absorbance bands of 1798–1812, 1425–1435, 876–874 and 712 cm^{-1} are assigned to asymmetric stretching carbonate group. Bands between 2545 and 2514 cm^{-1} represent the variation of Mg^{2+} or Ca^{2+}. The results are in good agreement with Bötcher et al. (1997) and Gunasekaran and Anbalagan (2007).

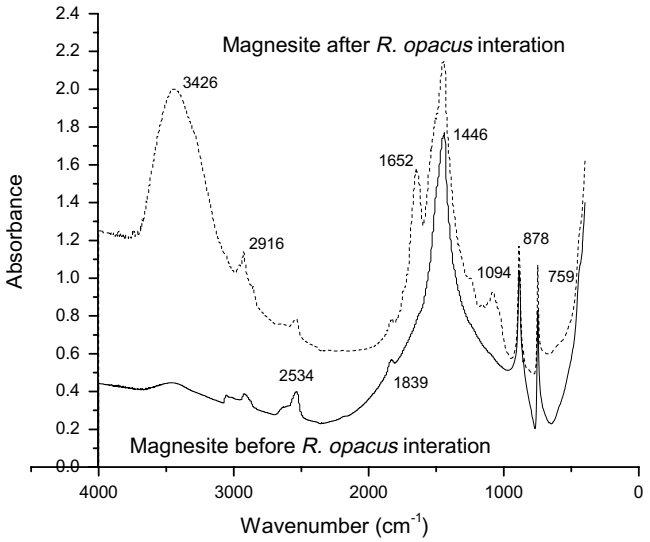

Fig. 3. FTIR spectra of magnesite and the principal bands obtained before and after of *R. opacus* interaction.

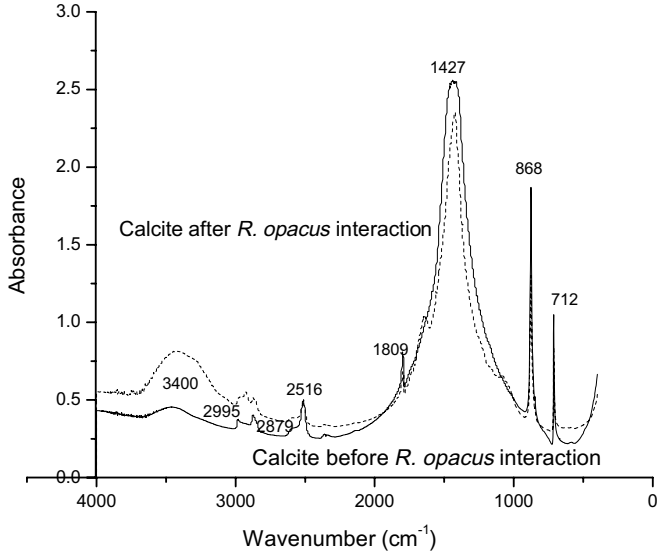

Fig. 4. FTIR spectra of calcite and the principal bands obtained before and after of *R. opacus* interaction.

The FTIR spectra of magnesite, after *R. opacus* interaction, exhibited some modifications comparing with the initial results. Absorbance bands (cm^{-1}) of 3400 assigned to hydroxyl groups (OH and NH), 2916 assigned to CH_3, 1632 assigned to amide and 1094 assigned to amines groups may be associated with functional groups presented on the *R. opacus* cell wall and could interact with the magnesite surfaces.

Comparing Fig. 3 with the FTIR spectra of calcite after *R. opacus* interaction (Fig. 4), it is observed as the calcite spectra suffers minor modifications than the magnesite spectra, however it can observe the absorbance band of 3400 and 2995 cm^{-1} that is associated with hydroxyl (OH and NH) and CH_3 groups, respectively, may interact with the calcite surface.

Santhiya et al. (2002) compared the FTIR spectra of spharelite and galena after the *B. polymyxa* exopolysaccharides (ECP) interaction. The spharelite presented low affinity for the ECP and the FTIR spectra presented minor modifications. On the other hand, galena presented better affinity for the ECP and the FTIR spectra suffers significant modifications.

The results obtained in the FTIR study are in good agreement with the mineral zeta potential modification, where it is observed a better affinity of the *R. opacus* cells for the magnesite surface than calcite. Sharma and Hunumantha (2003) found differences in the zeta potential profiles between *Acidithiobacillus ferroxidans* cells and the results were completed with the FTIR analysis.

3.3. Microflotation studies

The floatability studies were performed in order to evaluate the potential use of *R. opacus* as a biocollector. Based on the most favorable adsorption results found in previous studies, three pH values were selected for use in the flotation tests (Botero et al., 2006).

Figs. 5 and 6 show the floatability results of magnesite as function of the *R. opacus* concentration.

The results obtained in the magnesite flotation experiments (Fig. 5), for the studied pH range, suggests that the *R. opacus* adsorption on the magnesite surface improves its floatability. The best floatability was around 92% for a 100 ppm of *R. opacus* as biocollector at pH around five. According to Stratton et al. (2002), the lipids contained in the cell walls of *R. opacus* include free lipid, glicolipid, phospholipid and the carboxyl groups that would present affinity for the minerals surfaces. Moreover, Beveridge and Murray (1976) and Fein et al. (1997) found that some functional groups of gram positive bacteria have an affinity for certain metal ions, which leads to metal binding. The results may suggest that Mg sites play a similar

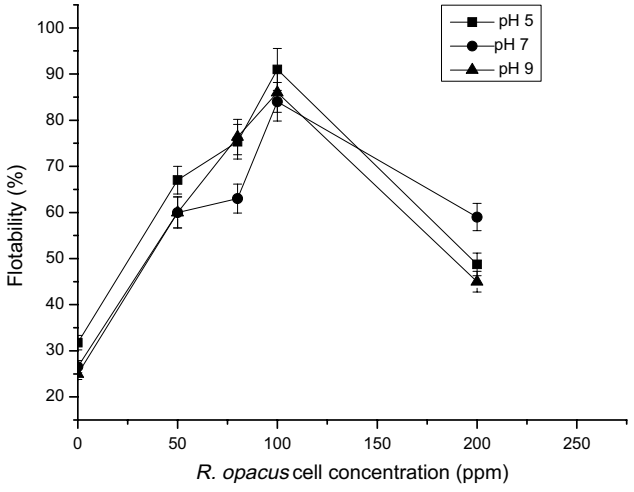

Fig. 5. Floatability of magnesite as function of *R. opacus* concentration for different pH values.

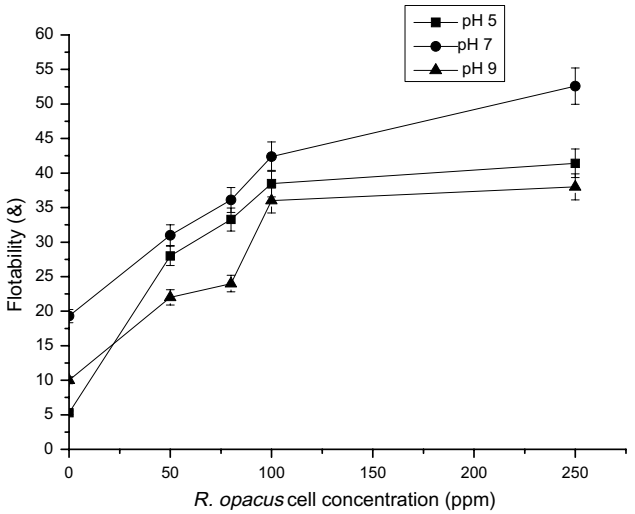

Fig. 6. Floatability of calcite as function of *R. opacus* concentration for different pH 7 values.

and important role for the adsorption of the bacteria onto magnesite surface. Gawel et al. (1997) studied the effect of the biotreatment on the flotation recovery of magnesite tailings using *A. niger*. As it was suggested in the Gawel et al.'s study (1997), the complex formation between metabolites and surface species can be considered as an adsorption mechanism of the *R. opacus* on the magnesite surface.

It was observed that the highest floatability is achieved for a *R. opacus* concentration of 100 ppm. Beyond this value, the floatability decreases. The fact is apparently due to the very large magnesite flocks formed that cannot be levitated by the gas bubbles. The results suggest a *R. opacus* critical concentration where the micro-organism would reduce their collector capacity. Dubel et al. (1992) found similar results using the *Mychobacterium phlei* as collector in the hematite flotation.

Fig. 6 shows the floatability results of calcite using *R. opacus* as biocollector. The pH values were selected based on the best affinity of the micro-organism for the minerals surfaces, previously evaluated in the adsorption tests (Botero et al., 2006).

The flotation results for calcite (Fig. 6) showed that the floatability was lower than magnesite; nevertheless, the results showed as the *R. opacus* collector improved the floatability of the mineral. The best biofloatability results for calcite achieved values around 55% for a *R. opacus* concentration of 220 ppm in pH around 7.0.

Flotation of calcite would be facilitated by bacterial interaction. The biopolymers, present in the *R. opacus* cell wall, contain some exopolysaccharides which could interlink the mineral particles though polymer binding and modify the mineral surface (Natarajan, 2006; Pavlovic and Brandão, 2003; Subramanian et al., 2003).

Others biofloatation studies have been carried out with the carbonate minerals. Zheng et al. (2001) studied the effect of the bacteria *B. subtillis* onto dolomite and apatite. They found that *B. subtillis* had more affinity for the dolomite than to apatite surface. It is probably that the better binding to dolomite could related to the magnesium sites on the dolomite surfaces.

3.4. DLVO and X-DLVO theories and thermodynamic approach studies

The interaction energies between *R. opacus* and the mineral surfaces were estimated comparing the classical DLVO theory with the X-DLVO.

Table 4 shows the contact angles measurements using the α-bromonapthalene as an apolar solvent, the γ_s^d components, the individual Hamaker constant for *R. opacus*, calcite and magnesite and the effective Hamaker constant for the bacteria–water–mineral system.

The interfacial tension value obtained for *R. opacus* for this study is in agreement with Christofi and Ivshina (2002). They measured the interfacial tension for different *Rhodococcus* strain and found that the interfacial tension value were between 0 and 9 mJ m^2.

The interfacial tension values obtained for magnesite and calcite were compared with the values of Wu and Nancollas (1999) and based on the Médout-Marère et al. studies (1998). They calculate the interfacial tension of several surface minerals using different methods and found a good approach with the apolar and polar liquids and the contact angle method.

Table 5 shows the interfacial components for *R. opacus*, calcite and magnesite and the. ΔG_{adh} for the bacteria–mineral systems using Eqs. (6), (7) and (9).

Using the thermodynamic approach and analyzing the ΔG_{bwm}^{LW}, ΔG_{bwm}^{AB}, ΔG_{bwm}^{adh} for the calcite and magnesite system, it is interesting to observe how the total free energy value of adhesion of *R. opacus* on magnesite is more negative than

Table 4
The contact angles measurements, the individual Hamaker constant for *R. opacus*, calcite and magnesite and the effective Hamaker constant for the bacteria–water–mineral system

Material	Angle contact (θ) α-bromo-naftalene	Interfacial tension γ_s^d (mJ m^{-2})	Hamaker constant (J)	Effective Hamaker constant (J)
R. opacus	15	0.64	9.23×10^{-22}	–
Calcite	16.4	0.79	8.46×10^{-22}	2.64×10^{-20}
Magnesite	2	3.78	5.45×10^{-21}	1.92×10^{-20}

Table 5
Interfacial components for *R. opacus*, calcite and magnesite and the ΔG_{adh} for the bacteria–mineral systems

Component	γ^{LW} (mJ m^{-2})	$\gamma+$ (mJ m^{-2})	$\gamma-$ (mJ m^{-2})	ΔG_{bwm}^{LW} (mJ)	ΔG_{bwm}^{AB} (mJ)	ΔG_{bwm}^{adh} (mJ)
R. opacus	0.64	8.12	28.51			
Water	21.8	25.5	25.5			
Calcite	0.59	5.69	57.02	6.26	−0.77	−7.03
Magnesite	3.78	51.14	9.45	13.24	−18.26	−32.20

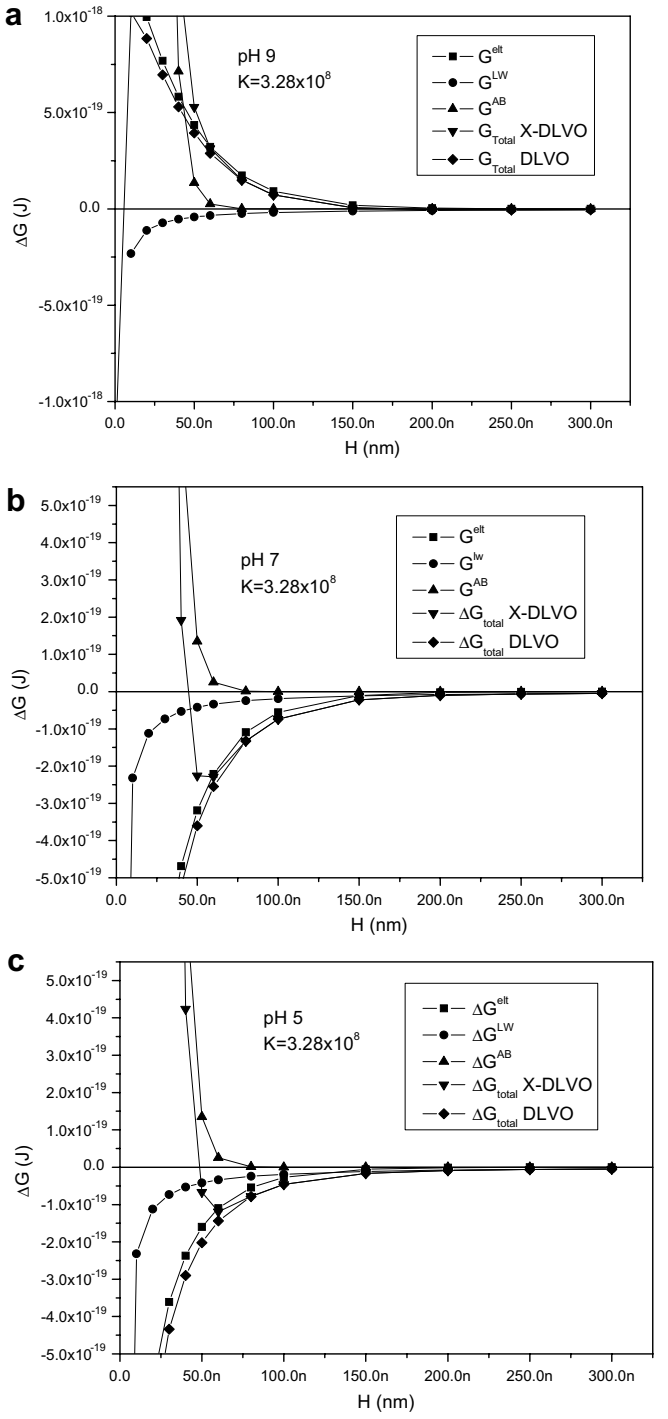

Fig. 7. DLVO and X-DLVO theories applied to *R. opacus* – magnesite–water system: (a) pH 5, (b) pH 7 and (c) pH 9.

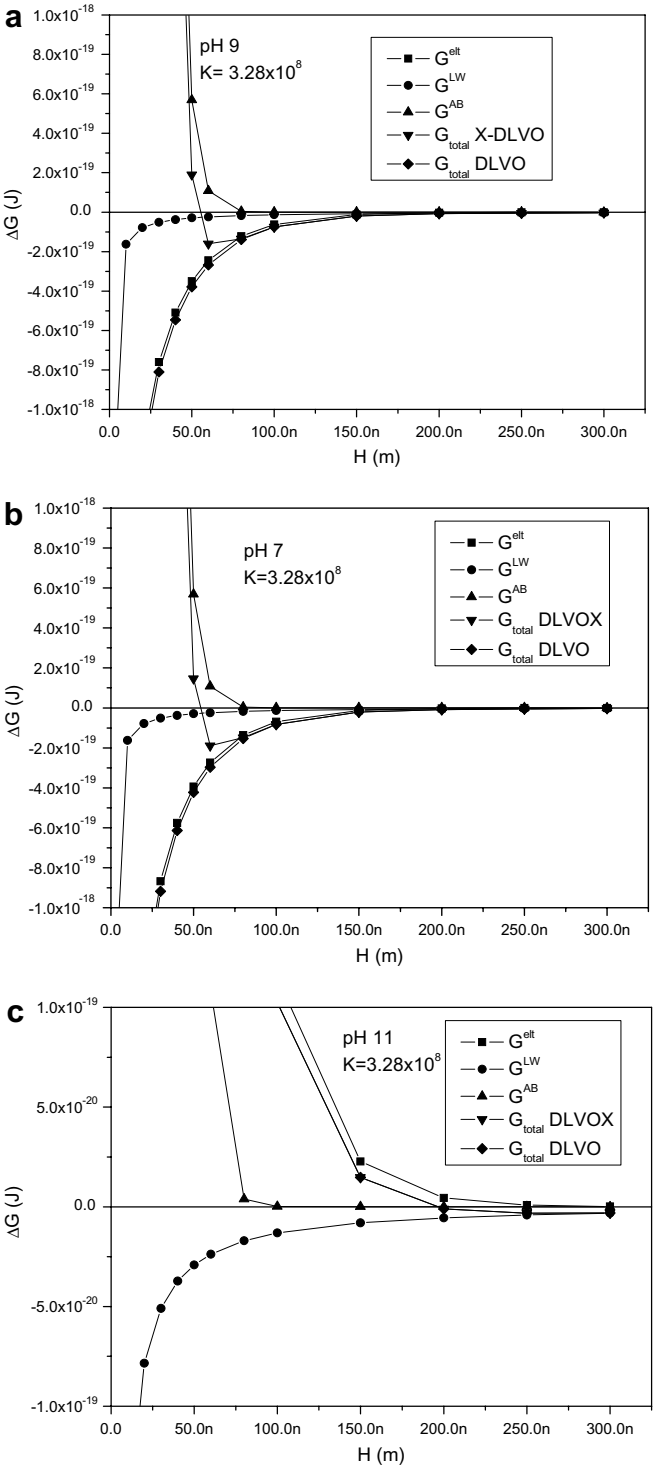

Fig. 8. DLVO and X-DLVO theories applied to *R. opacus* – calcite–water system: (a) pH 9, (b) pH 7 and (c) pH 5.

calcite system. Therefore, the approach predicts that there would be a better adhesion of *R. opacus* on magnesite than on the calcite surface.

The total interaction energy for *R. opacus* – water–calcite and *R. opacus* – water–magnesite system were calculated using the classic DLVO and X-DLVO theories. Figs. 7 and 8 show the ΔG^{elt}, ΔG^{atr}, ΔG^{AB}, DLVO ΔG_{total} and X-DLVO ΔG_{tot} and as function of the distance (H) for magnesite and calcite, respectively.

The adhesion of bacterial cells on the mineral surfaces could be possible when the bacterial cells and minerals particles are oppositely charged the electrostatic and the acid–base interactions cause the formation of a secondary

minimum. Comparing Figs. 7 and 8, at pH 5 and pH 7 for magnesite and calcite systems, one can realize that the secondary minimum for magnesite is deeper than calcite suggesting a stronger interaction between the *R. opacus* and the magnesite at pH 9 for magnesite and pH 11 for calcite, the charges of *R. opacus* and the mineral surfaces are the same and the adhesion is not favorable. The X-DLVO and DLVO curves are in agreement with the thermodynamic approach and the adhesion test made previously by Botero et al. (2006).

Still the bacterial interaction onto the mineral surface is not clear, many theories as the DLVO–X-DLVO and thermodynamic approach have been used with the aim to predict the adhesion mechanism. Sharma and Hunumantha Rao (2002) and Vijayalaskhmi and Raichur (2003) considered the total free energy of the interaction surfaces including the Lifshitz–van der Waals forces, electrostatic forces and acid–base interaction. Other properties as the roughness and the cell geometry have not yet considered due to some experimental evaluation and confidence on the results. These considerations could help to have a better understanding of the total interaction mechanism between the *R. opacus* and the carbonate mineral surface.

4. Conclusions

The zeta potential evaluation before and after the *R. opacus* interaction shows as the micro-organism modifies the reversal charge of calcite and magnesite, the IEP of both minerals were shifted to the left. The FTIR *R. opacus* spectra are in agreement with the zeta potential and the cell wall composition results, where the IEP reflects a combination of with NH_3^+ polymers and low pKa anionic polysaccharides with phosphate and carboxyl groups.

The FTIR spectra of magnesite after *R. opacus* interaction exhibit absorbance bands corresponding to CH_3, amide and amines groups that may be associated with functional groups present on the *R. opacus* cell wall and could interact whit the magnesite surfaces. The calcite spectra exhibits minor modifications than the magnesite results.

The most remarkable biofloatability results for magnesite and calcite achieved, respectively, values around 93% for a *R. opacus* concentration of 100 ppm in the pH around 5.0% and 55% for *R. opacus* concentration of 220 ppm in the pH around 7.0.

Using the thermodynamic approach the results show that the total free energy value of adhesion of *R. opacus* on magnesite is more negative than calcite system, therefore the approach predicts that there would be more affinity of *R. opacus* for magnesite than by the calcite surface. Comparing the X-DLVO curves with DLVO curves, it is observed the minimum secondary for magnesite is deeper than calcite confirming the better interaction between the *R. opacus* and the magnesite. The surface chemistry studies for *R. opacus* are an innovated tool to understand the interactions mechanisms with the carbonate minerals.

Acknowledgments

The authors acknowledge Professor José Farias de Oliveira, UFRJ and Professor Maria Isabel Paes da Silva, PUC-Rio for their support on the FTIR and contact angle experiments and CNPq, CAPES and FAPERJ for the financial support.

References

Beveridge, T.J., Murray, R.G., 1976. Uptake and retention of metals by cell walls of *Bacillus subtilis*. Journal of Bacteriology 127 (3), 1502–1518.

Bötcher, M.E., Gehlken, P.L., Steele, F., 1997. Characterization of inorganic and biogenic magnesian calcites by Fourier transform infrared spectroscopy. Solid State Ionics 101–103, 1379–1385.

Botero, A.E., Torem, M.L., Mesquita, L.M.S., 2006. Bioflotation of calcite and magnesite using *Rhodococcus opacus*. In: Proceedings of Reagents, 2006, Cape Town, CD-ROM.

Botero, A.E., Torem, M.L., Mesquita, L.M.S., 2007. Fundamental studies of *Rhodococcus opacus* as a biocollector of calcite and magnesite. Minerals Engineering 20, 1026–1032.

Cammarota, M.C., 1998. Exopolysaccharides production and microbial adhesion. PhD Thesis, UFRJ, Rio de Janeiro, Brazil (in Portuguese).

Chandaphara, M.N., Natarajan, K.A., Somasundaran, P., 2006. Surface chemical characterization of *Acidithiobacillus ferroxidans* grown in presence of different metal ions. In: Proceedings of the XXIII International Mineral Processing Congress IMPC, Istanbul, pp. 442–447.

Christofi, N., Ivshina, I.B., 2002. Microbial surfactants and their use in field studies of soil remediation. Journal of Applied Microbiology 93, 915–929.

Deo, N., Natarajan, K.A., 1997. Interaction of *Bacillus polymyxa* with some oxides minerals with reference to mineral beneficiation and environmental control. Minerals Engineering 10 (12), 1339–1354.

Deo, N., Natarajan, K.A., 1999. Role of corundum-adapted strains of *Bacillus polymyxa* in the separation of hematite and alumina. Minerals and Metallurgical Processing 16 (4), 29–34.

Deo, N., Natarajan, K.A., Somusundaran, P., 2001. Mechanisms of adhension of Paenibacillu polymixa onto hematite, corundum and quartz. International Journal of Mineral Processing 62, 27–39.

Dubel, J., Smith, R.W., Misra, M., Chen, S., 1992. Micro-organism as chemical reagents: the hematite system. Minerals Engineering 5 (3–5), 547–556.

Dubois, M., Gilles, K.A., Hamilton, J.K., Reberrs, P.A., Smith, F., 1956. Colorimetric method for determination of sugars and related substances. Analytical Chemistry 28, 350–355.

Fein, J.B., Daughney, C., Yee, N., Davis, T.A., 1997. A chemical equilibrium model for metal adsorption onto bacterial surfaces. Geochimica et Cosmochimica Acta 61 (16), 3319–3328.

Fröberg, J.C., Rojas, O.J., Cleason, P.M., 1999. Surface forces and measuring techniques. International Journal of Mineral Processing 56, 1–10.

Gawel, J., Maliszewska, I., Sadowski, Z., 1997. The effect of biopretreatment on the flotation recovery of magnesite tailings. Mineral Engineering 10 (8), 813–824.

Gunasekaran, A., Anbalagan, G., 2007. Spectroscopic characterization of natural calcite minerals. Spectrochimica Acta, Part A, 1733–1739.

Hermansson, M., 1999. The DLVO theory in microbial. Adhesion Colloids and Surfaces B: Biointerfaces 14, 105–119.

Hosseini, T.R., Kolahdoozan, M., Tabatabaei, Y.S.M., Oliazadeh, M., Noaparast, M., Eslami, A., Manafi, Z., Alfantazi, A., 2005. Bioflotation of Sarcheshmeh copper ore using *Thiobacillus ferroxidans* bacteria. Minerals Engineering 18 (3), 371–374.

Israelachvili, J., 1995. Intermolecular and Surface Forces, fifth ed. Academic Press, London.

Kwok, D.Y., Neumann, A.W., 1999. Contact angle measurement and contact angle interpretation. Advances in Colloid and Interface Science 81, 167–249.

Laskowski, J.S., Ralston, J., 1992. Colloid Chemistry in Minerals Processing. Elsevier, Amsterdam.

Lowry, O.H., Rosebrough, N.H., Farr, A.L., Randall, R.J., 1951. Protein measurement with the folin phenol reagent. Journal of Biological Chemistry 193, 265–275.

Médout-Marère, V., Malandrini, H., Zoungrana, T., Doullard, J.M., Pertyka, S., 1998. Thermodynamic investigation of surface minerals. Journal of Petroleum Science and Engineering 20, 223–231.

Mesquita, L.M.S., 2000. Selective studies of hematite and quartz bioflotation. PhD Thesis, PUC-Rio, Brazil (in Portuguese).

Mesquita, L.M., Lins, F.F., Torem, M.L., 2003. Interaction of a hydrophobic bacterium strain in a hematite–quartz floatation system. International Journal of Mineral Processing 71, 31–44.

Misra, M., Bukka, S., Chen, M., 1996. The effect of growth medium of *Thiobacillus ferrooxidans* on pyrite flotation. Minerals Engineering 9 (2), 157–168.

Natarajan, K.A., 2006. Microbially-induced mineral flotation and flocculation: prospects and challenges. In: Proceedings of the XXIII International Mineral Processing Congress IMPC, Istanbul, pp. 487–498.

Parker, F., 1971. Applications of Infrared Spectroscopy in Biochemistry. In: Biology and Medicine. Adam Hilger, London.

Patra, P., Natarajan, K.A., 2003. Microbially induced flocculation and flotation for separation of chalcopyrite from quartz and calcite. International Journal of Mineral Processing 74, 143–155.

Pavlovic, S., Brandão, P.R.G., 2003. Adsorption of starch amylase, amylopectin and glucose monomer and their effect on the flotation of hematite and quartz. Minerals Engineering 16, 1117–1122.

Pearse, M.J.N., 2005. An overview of the use of chemical reagents. Minerals Engineering 18, 139–149.

Pokrovsky, O., Schott, J., Thomas, F., 1999. Processes at the magnesium-bearing carbonates/solution interface. I. A surface speciation model for magnesite. Geochimica et Cosmochimica Acta 63 (6), 863–880.

Poortiga, A., Boss, R., Norde, W., Bussher, H., 2002. Electric double layer interactions in bacterial adhesion to surfaces. Surface Science Reports 47, 1–32.

Rijnaarts, H.M., Norde, W., Lyklema, J., Zehnder, A., 1995. The isoelectric point of bactéria as an indicator for the presence of cell surface polymers that inhibit adhesion. Colloids and Surfaces B: Biointerfaces 4, 191–197.

Santhiya, D., Subramanian, S., Natarajan, K.A., 2002. Surface chemical studies on spharelite and galena using extracellular polysaccharides isolated from *Bacillus polymyxa*. Journal of Colloid and Interface Science 256, 237–248.

Sharma, P.K., 2001. Surface studies relevant to microbial adhesion and biofloatation of sulphide minerals. Doctoral Thesis, Lulea University of Technology, Sweden.

Sharma, P.K., Hunumantha Rao, K., 2002. Analysis of different approaches for evaluation of surface energy of microbial cells by contact angle goniometry. Advances in Colloids and Interfaces Science 98, 341–463.

Sharma, P.K., Hunumantha Rao, K., 2003. Adhesion of *Paenibacillus polymyxa* on chalcopyrite and pyrite: surface thermodynamics and extended DLVO theory. Colloids and Surfaces B: Biointerfaces 29, 21–38.

Smith, R.W., Miettinem, M., 2006. Micro-organisms in flotation and flocculation: future technology or laboratory curiosity? Minerals Engineering 19, 548–553.

Stratton, H., Brooks, P., Griffiths, P., Seviour, R., 2002. Cell surface hydrophobicity and mycolic acid composition of *Rhodococcus* strains isolated from activated sludge foam. Journal of Industrial Microbiology and Biotechnology 28, 264–267.

Subramanian, S., Santhiya, D., Natarajan, K.A., 2003. Surface modification studies on sulphide minerals using bioreagents. International Journal of Mineral Process 72 (1–4), 175–188.

Van der Mei, H.C., Bos, R., Busscher, H.J., 1998. A reference guide to microbial cell surface hydrophobicity based on contact angles. Colloids and Surfaces B: Biointerfaces 11, 213–221.

Van der Wal, A., Norde, A., Zehnder, A.J.B., Lyklema, J., 1997. A determination of the total charge in the cell walls of gram-positive bacteria. Colloids and Surfaces B: Biointerfaces 9, 81–100.

Van Oss, C.J., 1994. Interfacial Forces in Aqueous Media. Marcel Dekker Inc., New York.

Van Oss, C.J., 1995. Hydrophobicity of biosurfaces–origin, quantitative determination and interaction energies. Colloids and Surfaces B: Biointerfaces 5, 91–110.

Vdovic, N., Bigdan, J., 1998. Electrokinetics of natural and synthetic calcite suspensions. Colloids and Surfaces: Physicochemical and Engineering Aspects 137, 7–14.

Vijayalaskhmi, S.P., Raichur, A.M., 2003. The utility of *Bacillus subtilis* as a bioflocculant for fine coal. Colloids and Surfaces B: Biointerfaces 29, 265–275.

Wu, W., Nancollas, G.H., 1999. Determination of interfacial tension from crystallization and dissolution data: a comparison with other methods. Advances in Colloid and Interface Science 79, 229–279.

Zheng, X., Arps, P.J., Smith, R.W., 2001. Adhesion of two bacteria onto dolomite and apatite: their effect on dolomite depression in anionic flotation. International Journal of Mineral Processing 62, 159–172.